

Photochemical Production of Hydroxyl Radical and Hydroperoxides in Water Extracts of  
Nascent Marine Aerosols Produced by Bursting Bubbles from Sargasso Seawater

Xianliang Zhou<sup>1</sup>, Andrew J. Davis<sup>2</sup>, David J. Kieber<sup>2</sup>, William C. Keene<sup>3</sup>, John R. Maben<sup>3</sup>, Hal  
Maring<sup>4</sup>, Elizabeth E. Dahl<sup>2,5</sup>, Miguel A. Izaguirre<sup>5</sup>, Rolf Sander<sup>7</sup>, and Linda Smoydzyn<sup>8,9</sup>

<sup>1</sup> Wadsworth Center, NYS Department of Health, and School of Public Health, SUNY at Albany,  
Albany, NY

<sup>2</sup> Chemistry Department, State University of New York, College of Environmental Science and  
Forestry, Syracuse, NY

<sup>3</sup> Department of Environmental Sciences, University of Virginia, Charlottesville, VA

<sup>4</sup> NASA, Radiation Sciences Program, Washington, DC

<sup>5</sup> Now at Chemistry Department, Loyola College in Maryland, Baltimore, MD

<sup>6</sup> Rosenstiel School of Marine and Atmospheric Science, University of Miami, Miami, FL

<sup>7</sup> Air Chemistry Department, Max Planck Institute for Chemistry, Mainz, Germany

<sup>8</sup> Institute for Environmental Physics, University of Heidelberg, Heidelberg, Germany

<sup>9</sup> Now at School of Environmental Sciences, University of East Anglia, Norwich, UK

Submitted to

*Geophysical Research Letters*

21 July 2008

1 **Abstract:** Marine aerosols produced by bursting bubbles at the ocean surface are highly enriched  
2 in organic matter (OM) relative to seawater. The importance of this OM in the photochemical  
3 evolution of marine aerosols and particularly as a source of reactive oxidants are unknown but  
4 likely significant. To investigate oxidant production, nascent aerosols were generated by bubbling  
5 zero air through flowing Sargasso seawater and photochemical production of OH radical and  
6 hydroperoxide were quantified in aqueous extracts exposed to solar radiation. Extrapolation to  
7 ambient conditions indicates that OM photolysis was the primary *in situ* source for OH ( $1.1 \times 10^{-8}$   
8  $\text{M s}^{-1}$ ) and hydroperoxides ( $1.7 \times 10^{-8} \text{ M s}^{-1}$ ) in nascent aerosols;  $\text{NO}_3^-$  photolysis was the primary  
9 source in aged, acidified aerosols ( $1.4 \times 10^{-7}$  and  $4.1 \times 10^{-8} \text{ M s}^{-1}$ , respectively). *In situ* OH  
10 photoproduction was comparable to gas-phase uptake whereas  $\text{H}_2\text{O}_2$  photoproduction was slower.  
11 Results provide important constraints for poorly quantified oxidant sources in marine aerosols.

## 13 **Introduction**

14 Breaking waves on the ocean surface produce bubbles that, upon bursting, inject seawater  
15 constituents into the atmosphere [Blanchard and Woodcock, 1980]. In terms of mass flux, this is the  
16 dominant source of atmospheric aerosols over most of Earth's surface [Lewis and Schwartz, 2004].  
17 Chemical processing of aerosols in the marine boundary layer (MBL) significantly influences  
18 tropospheric chemistry including ozone formation [Dickerson *et al.*, 1999]; oxidation processes [Sander  
19 and Crutzen, 1996]; and sulfur cycling, radiation balance, and climate [von Glasow *et al.*, 2002].

20 The relative concentrations of inorganic constituents of nascent marine aerosols are similar to  
21 those in bulk seawater but OM is highly enriched (by two to three orders of magnitude) [Keene *et al.*,  
22 2007]. Photochemical transformations involving this OM are likely a major source of reactive  
23 species including the OH radical and hydroperoxides. This potentially large oxidant source is not  
24 considered in models [e.g., Erickson *et al.*, 1999; Sander *et al.*, 2005] but may have important  
25 implications for multiphase processing of halogens, sulfur, nitrogen and other reactive constituents  
26 in the MBL.

27 The nature and magnitude of potential impacts of nascent marine aerosols are uncertain  
28 because they are injected into the atmosphere already populated with primary aerosols that  
29 originate from non-marine sources (crustal dust, combustion-derived elemental carbon, etc.) and  
30 associated reaction products, and secondary aerosols produced via nucleation and growth pathways.  
31 In addition, nascent aerosols in the MBL undergo rapid (seconds) multiphase chemical and physical

32 transformations. Consequently, it is virtually impossible to unequivocally characterize their  
33 properties based on measurements of aerosol composition in ambient air. To overcome this  
34 limitation, we designed and deployed a novel high-capacity aerosol generator to investigate the  
35 characteristics and photochemical evolution of nascent marine aerosols. Here we report  
36 photochemical production rates of the OH radical and hydroperoxides in water extracts of nascent  
37 aerosol produced in the generator and discuss factors that may affect their photoproduction as the  
38 aerosols age in ambient air.

39

## 40 **Experimental**

41 During spring and autumn 2005, nascent marine aerosols were generated by bubbling  
42 zero (ultrapure) air through fresh flowing Sargasso Sea water in a closed, relative humidity-  
43 controlled, 20-cm diameter, Pyrex chamber deployed at the Bermuda Institute for Oceans  
44 Sciences [Keene *et al.*, 2007]. Seawater flowed from bottom to top (range of 4 to 10 L min<sup>-1</sup>),  
45 overflow ports maintained constant water depth of 133 cm, and the depth of the overlying  
46 headspace was 81 cm. Zero air was bubbled (range of 1.0 to 9.0 L min<sup>-1</sup>) through fine-porosity  
47 glass frits 100 to 130 cm below the air-water interface. Bubble sizes near the air-water interface  
48 ranged from about 200- to 600- $\mu$ m diameter. Aerosol-laden exhaust air was sampled through  
49 isokinetic ports at the top of the generator. The closed system precluded chemical modification  
50 of the aerosols between production and recovery. The generator was operated under slight  
51 positive pressure to avoid contamination from lab air. See Keene *et al.* [2007] for additional  
52 details and a schematic.

53 To accumulate sufficient sample for characterization and photochemical experiments,  
54 aerosols were collected in bulk over nominal 24-h periods on 90-mm diameter Teflon filters  
55 (Gelman, 2.0  $\mu$ m pore size), and subsequently extracted in 15 mL of high purity laboratory water  
56 (resistivity  $\geq$  18.2 M $\Omega$  cm). Water extracts (hereafter referred to extracts) were analyzed for  
57 soluble organic carbon (OC) by high-temperature combustion with a Shimadzu Model TOC-V  
58 CSH analyzer and for major organic and inorganic ionic species by ion chromatography [Keene  
59 *et al.*, 2007].

60 Photochemical experiments were conducted with the extracts. Since nascent marine  
61 aerosols in ambient air are rapidly (s to min) acidified and enriched in NO<sub>3</sub><sup>-</sup>, selected extracts  
62 were amended with 0.05 - 1 mM H<sup>+</sup> (J.T. Baker Ultrex HCl) and/or 0.4 mM NO<sub>3</sub><sup>-</sup> (NaNO<sub>3</sub>, J.T.

63 Baker,  $\geq 99.9\%$ ) prior to a photochemical experiment to determine the influence of these  
 64 parameters on oxidant production. Photochemical experiments were started within 3 h after  
 65 aerosol samples were extracted. Aliquots were transferred to sealed screw-cap 1-cm rectangular  
 66 quartz cells (Hellma,  $\sim 4.1$  mL volume) and exposed to sunlight in an aluminum-foil lined water  
 67 bath for 4 to 7 h. The actinic UV flux, temperature, and photoproduction rates of the OH radical  
 68 and hydroperoxides were quantified during each experiment.

69 The actinic UV flux within the quartz cells was quantified by nitrate and nitrite actinometry  
 70 employing the method outlined in *Jankowski et al.* [2000]; the response bandwidth (and peak  
 71 response wavelength) for these actinometers was 311-333 (322) and 325-377 (352) nm, respectively.

72 The photochemical production rate of the OH radical ( $P_{OH}$ ) and the pseudo first order  
 73 reaction rate constant ( $k'_{ns}$ ) of the OH radical with reactants in the extracts were measured using  
 74 the method of *Zhou and Mopper* [1990]. Briefly, sodium benzoate (BA, recrystallized from  
 75 water) was added to extracts over a concentration range of 0.1-1 mM to immediately react with  
 76 the photoproduced OH radical in competition with natural reactants to form, in part, salicylate  
 77 (SA). The SA was measured by flow injection analysis with fluorescence detection (Hitachi,  
 78 model L-7480) at  $\lambda_{ex}$  305 nm and  $\lambda_{em}$  410 nm. The SA production rate ( $P_{SA}$ ) was derived from  
 79 its initial and final concentrations ( $[SA]_i$  and  $[SA]_t$ ) and photolysis rate ( $j_{SA}$ ):

$$80 \quad P_{SA} = \frac{j_{SA} ([SA]_t - [SA]_i e^{-j_{SA}t})}{(1 - e^{-j_{SA}t})} \quad (1)$$

81 where  $j_{SA}$  was calculated from nitrate actinometry [*Jankowski et al.*, 2000].  $P_{OH}$  and  $k'_{ns}$  were  
 82 derived from the intercept and the linear slope of  $\frac{1}{P_{SA}}$  vs  $\frac{1}{k'_b}$ :

$$83 \quad \frac{1}{P_{SA}} = \frac{k'_{ns}}{f_{SA} P_{OH}} \frac{1}{k'_b} + \frac{1}{f_{SA} P_{OH}} \quad (2)$$

84 where  $f_{SA}$  is 0.17, the fraction of SA formed from the BA-OH reaction [*Zhou and Mopper*, 1990;  
 85 *Jankowski et al.*, 2000], and  $k'_b$  is the pseudo-first-order rate constant for the BA-OH reaction  
 86 calculated from the BA concentration and pH [*Zhou and Mopper*, 1990].

87 Hydroperoxides were measured by a modified fluorescence method based on *Kok et al.*  
 88 [1995]. Briefly, hydroperoxides (-OOH), including  $H_2O_2$  and organic peroxides, produced in the  
 89 exposed extracts were derivatized with p-hydroxyphenylacetic acid, catalyzed by peroxidase, to  
 90 form a highly fluorescent dimer. The dimer was quantified by flow-injection analysis employing

91 fluorescence detection (Hitachi F-1200) at  $\lambda_{\text{ex}}$  325 nm and  $\lambda_{\text{em}}$  405 nm. Prior to analysis,  
92 hydroperoxides in samples and blanks were derivatized in 3 mL Teflon vials at a solution pH of  
93 5.8. Derivatized samples were injected into a flow-injection system containing water as the  
94 carrier phase. The carrier pH was adjusted to 11 after the injector by flowing through Nafion  
95 tubing submerged in 30 wt% aqueous ammonia.

96

## 97 **Results and Discussion**

98 Photochemical production rates of the OH radical and hydroperoxides and the OH radical  
99 reaction rate constant in marine aerosol samples are summarized in **Table 1**. Rates were  
100 determined by normalizing rates in extracts to the expected rates in freshly generated marine  
101 aerosol containing 5 M  $\text{Na}^+$  (equivalent to water content at ~80% relative humidity [*Erickson et*  
102 *al.*, 1999]) under full noontime tropical sun during the summer solstice and assuming a  $\text{NO}_3^-$   
103 photolysis rate constant of  $3.0 \times 10^{-7} \text{ s}^{-1}$  [*Mopper and Zhou*, 1990]. This extrapolation is based  
104 on the assumption that measured production rates scale linearly with dilution. Several factors  
105 constrain the reliability of directly extrapolating results based on manipulation of dilute bulk-  
106 aerosol extracts to ambient aerosols: 1) Production rates in dilute aerosol extracts do not reflect  
107 the potential influences of electrolyte interactions in concentrated aerosol solutions, 2) for  
108 hydroperoxides, net production rates in extracts may not scale linearly with dilution, 3)  
109 production rate constants in low- and high-ionic-strength solutions may differ, 4) evaluation of  
110 production rates as functions of particle size was beyond the scope of this study, and 5) the  
111 photon flux measured in aerosol extracts does not account for the influence of scattering by  
112 ambient aerosol. Despite these limitations, results do provide useful insight concerning this  
113 important but poorly constrained area of marine tropospheric chemistry.

114 Mean photoproduction rates ( $\pm 1\sigma$ ) of the OH radical and hydroperoxides in freshly  
115 generated aerosol samples (i.e., no  $\text{NO}_3^-$ ) were  $1.1 \pm 0.6 \times 10^{-8} \text{ M s}^{-1}$  (n=12) and  $1.7 \pm 0.5 \times 10^{-8} \text{ M}$   
116  $\text{s}^{-1}$  (n=15), respectively. By comparison,  $P_{\text{OH}}$  is  $\sim 3 \times 10^{-12} \text{ M s}^{-1}$  [*Mopper and Zhou*, 1990] and  
117  $P_{\text{H}_2\text{O}_2}$  is  $\sim 2 \times 10^{-12} \text{ M s}^{-1}$  in surface waters of the Sargasso Sea [for review *Kieber et al.*, 2003],  
118 which are  $10^3$  to  $10^4$  times lower than rates observed in our marine aerosol samples. The much  
119 higher rates that we calculated for marine aerosols are likely due to the large enrichment of OM  
120 relative to seawater. Except for  $\text{NO}_3^-$ -rich polar waters, OM is the main source of the OH radical

121 and hydroperoxides in seawater [Mopper and Zhou, 1990].  $\text{NO}_3^-$  and  $\text{NO}_2^-$  were not detected in  
122 our nascent marine aerosols but OM was highly enriched (average enrichment factor of  $\sim 387$  for  
123 all samples [Keene *et al.*, 2007]). We infer that both the OH radical and hydroperoxides were  
124 produced from photosensitized reactions involving OM in nascent marine aerosols.

125 Photoproduction rates of the OH radical and peroxides in fresh aerosols decreased with  
126 exposure to sunlight during the first 2 h and then leveled off after 4-5 h of irradiation (**Figure 1**).  
127 Production rates of OH and peroxides were  $\sim 50\%$  higher if based on the first hour exposure  
128 compared to rates at 7 h. Decreased production rates were probably due to the photobleaching of  
129 organic chromophores through both their direct photolysis and reactions with oxidants.  
130 Photobleaching significantly reduced OH production rates in aerosol extracts whereas no  
131 significant photobleaching or reductions in rates are detected in seawater after 7 h of solar  
132 irradiation [Zhou and Mopper, 1990]. The faster photobleaching in extracts may be due to the  
133 fact that the photoproduced OH radical in marine aerosols will react primarily with the highly  
134 concentrated OM (see discussion below) whereas over 90% of the OH radical produced in  
135 seawater will react with bromide [Zafiriou, 1974; Zhou and Mopper, 1990], which is not  
136 significantly enriched in nascent marine aerosols [Keene *et al.*, 2007]. The reported  
137 photoproduction rates are average values based on 5- to 7-h exposures to sunlight and,  
138 consequently, likely underestimate initial rates in fresh aerosols by  $\sim 50\%$ .

139 Following injection into the atmosphere, nascent marine aerosols are rapidly (s to min)  
140 acidified to pH 3-5 through scavenging of gas-phase acids and aqueous-phase oxidation of acid  
141 precursors [Keene *et al.*, 1998; Erickson *et al.*, 1999]. Acidification of aerosol extracts from pH  
142 5.5 to less than 4.5 increased OH photoproduction rates from  $1.1 \times 10^{-8} \text{ M s}^{-1}$  to  $2.5 \times 10^{-8} \text{ M s}^{-1}$ ,  
143 respectively (**Table 1**). These results suggest that the OH radical is derived from the photolysis  
144 of chromophores with a  $\text{pK}_a$  of 4.5 - 5.5 (e.g., phenolic compounds) and that the protonated  
145 chromophores have higher quantum yields for the production of the OH radical compared to the  
146 dissociated species. This hypothesis is consistent with recent observations that aquatic dissolved  
147 OM photoreactivity and OH radical production increases with acidity [Molot *et al.*, 2005]. This  
148 trend is also generally consistent with the observation that OH photoproduction from OM in aged  
149 marine aerosols increased by a factor of  $\sim 9$  as pH decreased from 7 to 4.6 [Anastasio and  
150 Newberg, 2007]. However, at substantially lower pHs less than 4, OH photoproduction rates in  
151 both aged marine aerosols [Anastasio and Newberg, 2007] and in aged Arctic aerosols

152 [Anastasio and Jordan, 2004] decrease significantly whereas those in nascent aerosols evaluated  
153 during our experiment did not. The variation in pH dependence of OH production may reflect  
154 the different types of organic and inorganic chromophores in ambient aerosols of different ages  
155 and from different regions. In our study, the average  $P_{OH}$  of  $\sim 2.5 \times 10^{-8} \text{ M s}^{-1}$  for all  
156 acidification experiments between pH 3.0 and 4.5 probably represents a typical value for the  
157 midday OH photoproduction rate from organic chromophores in marine aerosols over the central  
158 North Atlantic Ocean during the first day of their atmospheric lifetime.

159 In contrast to the OH radical, the photoproduction rate of peroxides in our extracts was  
160 relatively constant, i.e., within  $\pm 10\%$ , over the pH range 3.0 - 5.5. The difference in the pH  
161 dependence of the photoproduction of the OH radical and peroxides suggests that different types  
162 of chromophores are responsible for producing these species. This finding is consistent with  
163 differences observed in the action spectrum for their photoproduction in seawater; the OH radical  
164 is produced mostly in the UV-B (290-320 nm) [Mopper and Zhou, 1990] while  $\text{H}_2\text{O}_2$  is produced  
165 in both the UV-B and UV-A (320-400 nm) [Kieber *et al.*, 2003].

166 The scavenging of  $\text{HNO}_3$  from the gas phase leads to high concentrations of  $\text{NO}_3^-$  in  
167 ambient marine aerosols (e.g., an average of 0.4 M at Bermuda during the spring [Keene *et al.*,  
168 2002]). To assess the potential importance of  $\text{NO}_3^-$  photolysis as a source of the OH radical and  
169 peroxides, we measured OH and peroxide photoproduction rates in fresh marine aerosol samples  
170 with added  $\text{NO}_3^-$ . The extrapolated OH production rate from photolysis of  $\text{NO}_3^-$  at 0.4 M is  $\sim 1.4$   
171  $\times 10^{-7} \text{ M s}^{-1}$ , similar to the predicted value of  $1.2 \times 10^{-7} \text{ M s}^{-1}$  using a  $\text{NO}_3^-$  photolysis rate  
172 constant of  $3 \times 10^{-7} \text{ s}^{-1}$  [Zhou and Mopper, 1990]. When acidified to a pH between 3.0 and 4.5,  
173 the extrapolated OH production rate from  $\text{NO}_3^-$  photolysis increased to  $1.9 \times 10^{-7} \text{ M s}^{-1}$  and was  
174 the dominant contributor to the overall OH production rate of  $2.2 \times 10^{-7} \text{ M s}^{-1}$  from both OM and  
175  $\text{NO}_3^-$  photolysis in an acidified marine aerosol containing  $\text{NO}_3^-$  (**Table 1**). The hydroperoxide ( $-\text{OOH}$ )  
176 production from  $\text{NO}_3^-$  photolysis was relatively small ( $\sim 1 \times 10^{-9} \text{ M s}^{-1}$ ). However, the  
177 synergistic effect from photolysis of both OM and  $\text{NO}_3^-$  significantly enhanced peroxide  
178 production to a total of  $4.1 \times 10^{-8} \text{ M s}^{-1}$ , probably as a result of secondary radical reactions with  
179 OM initiated by the OH radical generated from  $\text{NO}_3^-$  photolysis.

180 The OH photoproduction rates in acidified marine aerosols ( $\sim 2.5 \times 10^{-8} \text{ M s}^{-1}$  from OM  
181 only and  $\sim 2.2 \times 10^{-7} \text{ M s}^{-1}$  from OM and  $\text{NO}_3^-$  combined, **Table 1**), are comparable to rates of

182  $\sim 2.8 \times 10^{-7} \text{ M s}^{-1}$  determined in ambient Arctic aerosol samples collected at Alert, Canada,  
183 during the spring [Anastasio and Jordan, 2004] and  $\sim 1 \times 10^{-7} \text{ M s}^{-1}$  in ambient, super- $\mu\text{m}$ -  
184 diameter aerosols collected along the California coast [Anastasio and Newberg, 2007]. While  
185 the majority of the OH produced (59%) in the California samples was from  $\text{NO}_3^-$  photolysis, the  
186 remaining fraction was most likely from OM. By contrast, only  $\sim 10\%$  of the OH radical was  
187 derived from  $\text{NO}_3^-$  photolysis in the Arctic aerosol samples during the spring [Anastasio and  
188 Jordan, 2004], probably due to significant accumulation of photo-labile species such as  $\text{NO}_2^-$  and  
189 organic chromophores during the dark cold Arctic winter.

190 Hydroperoxide production rates in fresh marine aerosols ( $\sim 1.7 \times 10^{-8} \text{ M s}^{-1}$  from OM and  
191  $\sim 4.1 \times 10^{-8} \text{ M s}^{-1}$  from OM and  $\text{NO}_3^-$  combined) were substantially lower than reported  $\text{H}_2\text{O}_2$   
192 production rates in Arctic aerosol samples ( $\sim 2.5 \times 10^{-6} \text{ M s}^{-1}$ , [Anastasio and Jordan, 2004]).  
193 These differences likely reflect the large differences expected in the composition of the aerosols  
194 considered in the two studies. In contrast to fresh, purely marine aerosols evaluated in our  
195 investigation, the ambient Arctic samples correspond to an aged mixture of primary and  
196 secondary aerosol components originating from multiple natural and anthropogenic sources.

197 We determined the relative importance of *in situ* photoproduction of the OH radical and  
198 hydroperoxides in the marine aerosols versus uptake of these species from the gas phase (**Figure 2**).  
199 Uptake rates were calculated following Erickson *et al.* [1999] for ambient conditions at 25 °C and 1  
200 atm, and assuming a gas-phase concentration of  $1 \times 10^6 \text{ molecules cm}^{-3}$  for OH and  $1.1 \times 10^9$   
201  $\text{molecules cm}^{-3}$  (45 pptv) for  $\text{H}_2\text{O}_2$ , an accommodation coefficient of 0.18 for  $\text{H}_2\text{O}_2$ , a mean free  
202 path of 0.1  $\mu\text{m}$  for both OH and  $\text{H}_2\text{O}_2$ , and a Henry's Law constant of  $1.0 \times 10^5 \text{ M atm}^{-1}$  for  $\text{H}_2\text{O}_2$ .  
203 Given the large associated uncertainty [e.g., Sander *et al.*, 2003], uptake rates that correspond to  
204 accommodation coefficients for OH of 0.01 and 0.1 are depicted. For hydroperoxides, *in situ*  
205 photoproduction rates in the marine aerosols were less than the calculated uptake rates from the gas  
206 phase over the entire size range by two or more orders of magnitude, which suggests that *in situ*  
207 photoproduction is not an important source of hydroperoxides in nascent marine aerosols. This  
208 conclusion is not consistent with results reported by of Anastasio and Jordan [2004], which  
209 indicate that *in situ*  $\text{H}_2\text{O}_2$  photoproduction is not only a dominant  $\text{H}_2\text{O}_2$  source in aerosols but also  
210 the major source of  $\text{H}_2\text{O}_2$  in the air mass in the Arctic during the polar springtime. The higher *in*

211 *situ* H<sub>2</sub>O<sub>2</sub> photoproduction rates in the Arctic aerosols possibly results from the accumulation of  
212 organic and inorganic chromophores during the cold Arctic winter.

213 The *in situ* OH photoproduction rate from OM ( $\sim 2.5 \times 10^{-8} \text{ M s}^{-1}$ ) is similar to the uptake  
214 rate of OH from gas phase (e.g.,  $1.5 \times 10^{-8} \text{ M s}^{-1}$  at  $\alpha=0.01$  and  $1.1 \times 10^{-7} \text{ M s}^{-1}$  at  $\alpha=0.1$ ) for 1-  
215  $\mu\text{m}$ -diameter aerosols (**Figure 2**). When the combined photolytic production from both NO<sub>3</sub><sup>-</sup>  
216 and OM are considered ( $2.2 \times 10^{-7} \text{ M s}^{-1}$ ), the *in situ* production is the dominant OH source in  
217 larger size fractions of marine aerosols. Therefore, *in situ* OH photoproduction is an important  
218 OH source in marine aerosols and should be considered in models that evaluate the  
219 photochemical evolution of marine aerosols and their role in the marine atmosphere. It should be  
220 noted that OC enrichment factors increased substantially with decreasing size of nascent marine  
221 aerosols, from 10<sup>2</sup> to 10<sup>3</sup> for super- $\mu\text{m}$  diameter aerosols to 10<sup>4</sup> to 10<sup>5</sup> for sub- $\mu\text{m}$  diameter  
222 aerosols [Keene *et al.*, 2007]. Consequently, relative to rates for bulk aerosol samples reported  
223 herein, photoproduction rates of the OH radical and hydroperoxides from OM would be expected  
224 to be significantly higher in the sub- $\mu\text{m}$  aerosol size fractions and therefore their relative  
225 contribution to the evolution of these aerosols is expected to be proportionately greater.

226 The OH radical reacts rapidly in marine aerosols. The observed pseudo first order rate  
227 constant ( $6.2 \pm 2.1 \times 10^8 \text{ s}^{-1}$ , **Table 1**) results in a lifetime of  $\sim 1.6 \times 10^{-9} \text{ s}$ , which is at the lower  
228 end of the range  $1.4 \times 10^{-9}$  to  $16 \times 10^{-9} \text{ s}$  reported for aged marine aerosols along the California  
229 coast [Anastasio and Newberg, 2007]. Assuming a total OH source strength of  $\sim 3.2 \times 10^{-7} \text{ M s}^{-1}$   
230 from *in situ* photoproduction ( $2.2 \times 10^{-7} \text{ M s}^{-1}$ ) and uptake from the gas phase ( $\sim 1 \times 10^{-7} \text{ M s}^{-1}$ ),  
231 the steady-state concentration of the OH radical in 1- $\mu\text{m}$ -diameter aerosols would be  $5.2 \times 10^{-16}$   
232 M, which is similar to the value of  $3.8 \times 10^{-16} \text{ M}$  calculated for aged super- $\mu\text{m}$  marine aerosols  
233 [Anastasio and Newberg, 2007] but approximately two orders of magnitude greater than that  
234 observed in surface seawater [Mopper and Zhou, 1990]. Reaction with Br<sup>-</sup> is the dominant sink  
235 for the OH radical in seawater, consuming more than 90% of the OH radical that is  
236 photochemically produced [Zafiriou, 1974; Zhou and Mopper, 1990]. Bromide is conservative  
237 during aerosol production [Keene *et al.*, 2007] and the Br<sup>-</sup> concentration in fresh aerosol at 80%  
238 RH is  $\sim 8 \text{ mM}$  accounting for  $\sim 13\%$  of the observed OH radical loss in fresh marine aerosols.  
239 Reaction with Cl<sup>-</sup> is also a minor OH sink in the marine aerosols. The rate constant increases  
240 with decreasing pH from  $\sim 3 \times 10^7 \text{ s}^{-1}$  ( $\sim 5\%$  of the observed OH loss rate) at pH 6 to  $\sim 1 \times 10^8 \text{ s}^{-1}$

241 (15% of the observed OH loss rate) at pH 3, as a result of acid-catalyzed decomposition of the  
242 intermediate product (ClOH) to Cl and OH<sup>-</sup> [*Anastasio and Newberg, 2007*]. Reactions of OH  
243 with halides, especially at lower pH, lead to formation of photo-labile halogen species such as  
244 Cl<sub>2</sub>, Br<sub>2</sub> and BrCl that influence oxidation processes in marine air.

245         The highly enriched OM in marine aerosols plays a dual role being an important  
246 precursor/source and a dominant sink for the OH radical, leading to degradation of OM and  
247 likely production of a suite of low-molecular weight (LMW) organic compounds. Less-volatile  
248 LMW products, such as di-carboxylic acids [*Kawamura and Sakaguchi, 1999*], would  
249 accumulate in marine aerosols contributing to aerosol acidification and modifying the  
250 physiochemical and optical properties of the aged aerosols. More volatile LMW products, such  
251 as carboxylic acids, ketones, and alcohols would partition into the gas phase and influence the  
252 multiphase chemical and photochemical evolution of the marine troposphere.

253

#### 254 **Acknowledgments**

255         We thank two anonymous reviewers for helpful comments and the Bermuda Institute for  
256 Ocean Sciences for outstanding logistical support during the field deployments. This research  
257 was supported by grants from the National Science Foundation, ATM-0343082 (HM), ATM-  
258 0343146 (WK), ATM-0343181 (XZ), and ATM-0343199 (DJK).

259 **References**

- 260 Anastasio, C. and A. L. Jordan (2004), Photoformation of hydroxylradical and hydrogen  
261 peroxide in aerosol particles from Alert, Nunavut: implications for aerosol and snowpack  
262 chemistry in the Arctic, *Atmos. Environ.* 38, 1153–1166.
- 263 Anastasio, C. and J. T. Newberg (2007), Sources and Sinks of hydroxyl radicals in sea-salt  
264 particles, *J. Geophys. Res.*, 112, doi:10.1029/2006JE002878.
- 265 Dickerson, R. R., K. P. Rhoads, T. P. Carsey, S. J. Oltmans, J. P. Burrows, and P. J. Crutzen  
266 (1999), Ozone in the remote marine boundary layer: A possible role for halogens, *J.*  
267 *Geophys. Res.*, 104, 21385-21395.
- 268 Erickson, D. J., C. Seuzaret, W. C. Keene, and S.-L. Gong (1999), A general circulation model  
269 based calculation of HCl and ClNO<sub>2</sub> production from sea-salt dechlorination: Reactive  
270 Chlorine Emissions Inventory, *J. Geophys. Res.*, 104, 8347-8372.
- 271 Jankowski, J. J., D. J. Kieber, K. Mopper and P. J. Neale (2000), Development and  
272 intercalibration of ultraviolet solar actinometers, *Photochem. Photobiol.*, 71, 431-440.
- 273 Kawamura, K., and F. Sakaguchi (1999), Molecular distributions of water soluble dicarboxylic  
274 acids in marine aerosols over the Pacific Ocean including tropics, *J. Geophys. Res.*, 104,  
275 3501–3509.
- 276 Keene, W. C., R. Sander, A. A. P. Pszenny, R. Vogt, P. J. Crutzen, and J. N. Galloway (1998),  
277 Aerosol pH in the marine boundary layer: A review and model evaluation, *J. Aerosol Sci.*,  
278 29, 339-356.
- 279 Keene, W. C., A. A. P. Pszenny, J. R. Maben, and R. Sander (2002), Variation in marine aerosol  
280 acidity with particle size, *Geophys. Res. Lett.*, 29(7), 1101, doi:10.1029/2001GL013881.
- 281 Keene, W. C., et al. (2007), Chemical and physical characteristics of nascent aerosols produced  
282 by bursting bubbles at a model air-sea interface, *J. Geophys. Res.*, 112,  
283 doi:10.1029/2007JD008464.
- 284 Kieber, D.J., B.M. Peake, and N.M. Scully (2003), Reactive oxygen species in aquatic  
285 ecosystems. In: *UV Effects in Aquatic Organisms and Ecosystems*. E.W. Hebling and H.  
286 Zagarese (Eds.). *Comprehensive Series in Photosciences* (D-P. Häder and G. Jori (Series  
287 Eds.). European Society for Photobiology. pp. 251-288.
- 288 Kok, G. L., S. E. McLaren, and T. A. Staffelbach (1995), HPLC Determination of Atmospheric  
289 Organic Hydroperoxides. *J. Atmos. Ocean. Technol.*, 12, 282-290.

290 Molot, L. A., J. J. Hudson, P. J. Dillon, and S. A. Miller (2005), Effect of pH on photo-oxidation  
291 of dissolved organic carbon by hydroxyl radicals in a coloured, softwater stream, *Aquat.*  
292 *Sci.*, 67, 189-195.

293 Mopper, K., and X. Zhou (1990), Photoproduction of hydroxyl radicals at the sea surface and its  
294 potential impact on marine processes. *Science*, 250:661-664.

295 Sander, R., and P. J. Crutzen (1996), Model study indicating halogen activation and ozone  
296 destruction in polluted air masses transported to the sea, *J. Geophys. Res.*, 101, 9121-9138.

297 Sander, S.P., et al. (2003), Chemical Kinetics and Photochemical Data for Use in Atmospheric  
298 Studies, Evaluation Number 14, JPL Publication 02-25. Jet Propulsion Laboratory,  
299 Pasadena.

300 Sander, R., A. Kerkweg, P. Jöckel, and J. Lelieveld, (2005), Technical Note: The new  
301 comprehensive atmospheric chemistry module MECCA, *Atmos. Chem. Phys.*, 5, 445–450.

302 von Glasow R, R. Sander, A. Bott, and P. J. Crutzen (2002), Modeling halogen chemistry in the  
303 marine boundary layer. 2. Interactions with sulfur and cloud-covered MBL, *J. Geophys.*  
304 *Res.*, 107, 4323, doi:10.1029/2001JD000943.

305 Zafiriou, O. C. (1974), Sources and reactions of OH and daughter radicals in seawater, *J.*  
306 *Geophys. Res.*, 79, 4491-4497.

307 Zhou, X., and K. Mopper (1990), Determination of photochemically produced hydroxyl radicals  
308 in seawater and freshwater, *Mar. Chem.*, 30, 71-88.

309 **Table 1.** Production rates of hydroperoxides ( $-OOH$ ) and OH ( $P_{OH}$  and  $P_{-OOH}$ , in  $M s^{-1}$ ) and reaction  
310 rate constant of OH with natural scavengers ( $k_{ns}$ , in  $s^{-1}$ ) are normalized to tropical solar noon during  
311 the summer solstice at  $\sim 80\%$  RH ( $Na^+$  concentration of 5 M). The median, arithmetic mean, standard  
312 deviation ( $\sigma$ ) and number of individual determinations (N) for each are listed. The potential influence  
313 of scattering on irradiance of ambient aerosols is not considered. Production rates from  $NO_3^-$   
314 photolysis are extrapolated to a  $NO_3^-$  concentration of 0.4 M. Light-based rates ( $M (Einstein\ cm^{-2})^{-1}$ )  
315 are given in parentheses; for  $-OOH$  and OH, rates are based on nitrite and nitrate actinometry,  
316 respectively. Enrichment factor of OC ( $EF_{OC}$ ) is defined as  $\frac{[OC_{aerosol}]/[Mg^{2+}_{aerosol}]}{[OC_{seawater}]/[Mg^{2+}_{seawater}]}$ .

Parameter	Median	Mean	$\sigma$	N
$P_{-OOH} OM^a$	$1.6 \times 10^{-8}$	$1.7 \times 10^{-8}$ (1.3)	$4.9 \times 10^{-9}$ (0.3)	15
$P_{-OOH} NO_3^-^b$		$9.5 \times 10^{-10}$ (0.1)		2
$P_{-OOH} OM+NO_3^-^c$		$4.1 \times 10^{-8}$ (6.0)		1
$P_{OH} OM^a$	$7.6 \times 10^{-9}$ (1.8)	$1.1 \times 10^{-8}$ (2.2)	$6.1 \times 10^{-9}$ (1.2)	13
$P_{OH} NO_3^-^b$	$1.4 \times 10^{-7}$ (29.7)	$1.4 \times 10^{-7}$ (29.6)	$1.6 \times 10^{-8}$ (3.5)	4
$P_{OH} OM\ acidified^d$	$2.5 \times 10^{-8}$ (5.8)	$2.5 \times 10^{-8}$ (7.5)	$1.8 \times 10^{-8}$ (6.0)	5
$P_{OH} (NO_3^-)\ acidified^d$	$1.9 \times 10^{-7}$ (39.6)	$1.9 \times 10^{-7}$ (41.2)	$1.0 \times 10^{-7}$ (21.9)	6
$P_{OH} (OM+NO_3^-)\ acidified^d$		$2.2 \times 10^{-7}$ (48.7)		
$k_{ns}$	$5.7 \times 10^8$	$6.2 \times 10^8$	$2.1 \times 10^8$	5
$EF_{OC}$	387	450	80	23

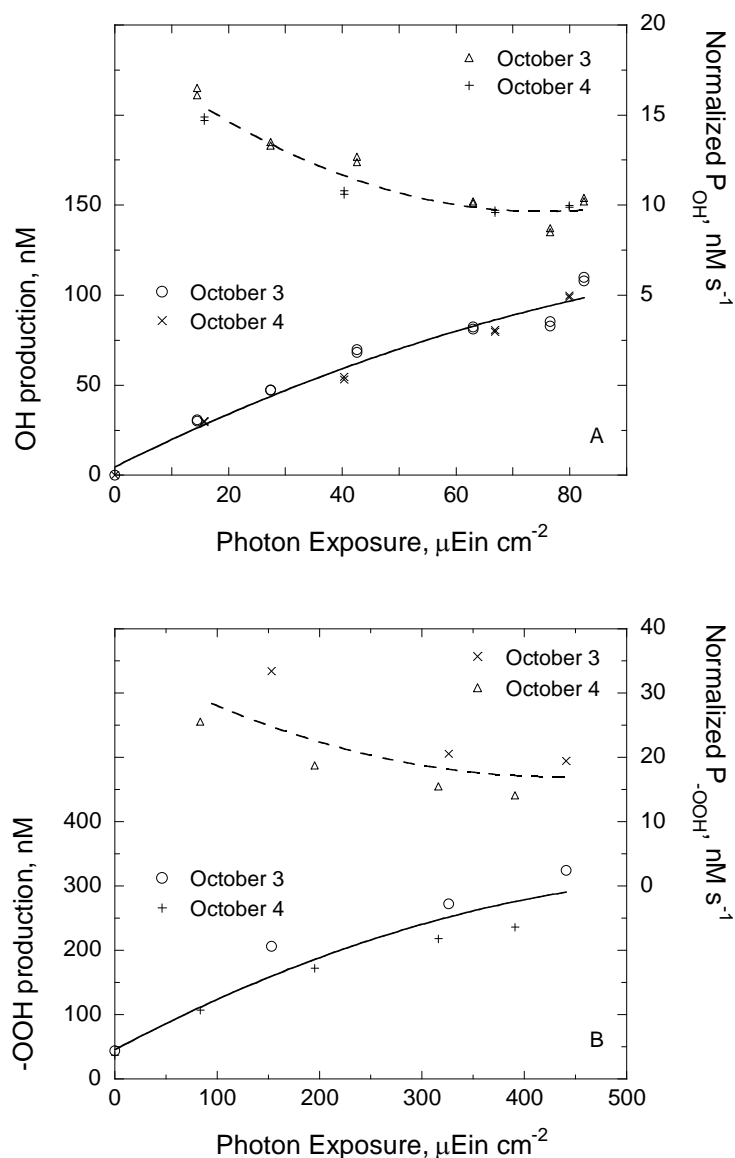
317 <sup>a</sup> production rates of OH and  $-OOH$  from the photolysis of OM in fresh aerosols (circumneutral pH  
318 and no  $NO_3^-$ ).

319 <sup>b</sup> production rates of OH and  $-OOH$  from  $NO_3^-$  photolysis (circumneutral pH).

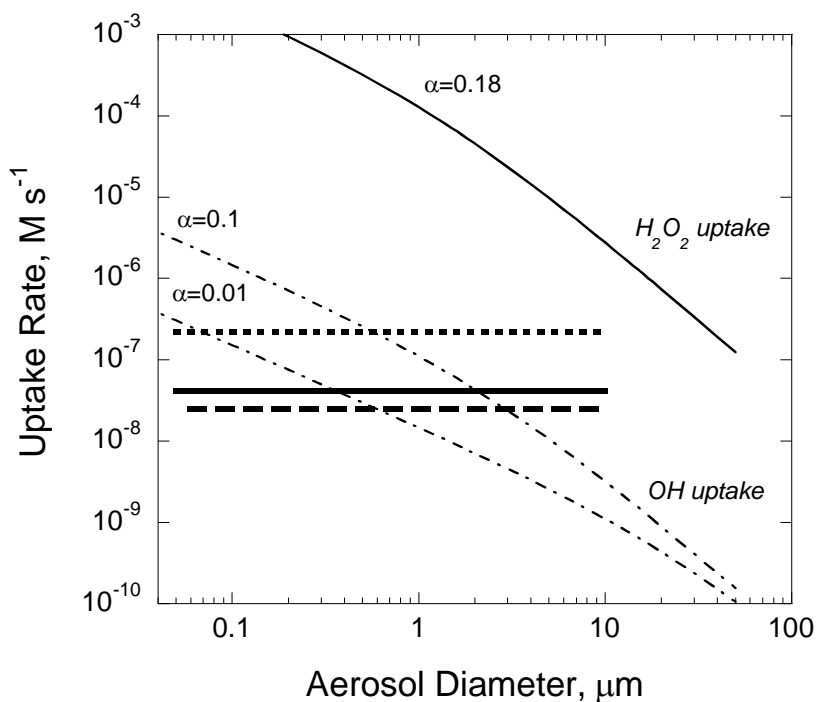
320 <sup>c</sup>  $-OOH$  production rate from the photolysis of  $OM + NO_3^-$  (circumneutral pH).

321 <sup>d</sup> OH production rates from the photolysis of OM,  $NO_3^-$  or  $(OM + NO_3^-)$  in acidified marine  
322 aerosols, respectively.

323



324  
 325 **Figure 1.** Production of OH radical and -OOH in aerosol extract (solid lines, left Y-axis) and  
 326 normalized photoproduction rates of OH and -OOH ( $P_{OH}$  and  $P_{-OOH}$ ) in marine aerosols (dashed lines,  
 327 right axis) as a function of photon exposure during a solar irradiation experiment. The photon  
 328 exposure for panels A and B were determined from nitrate and nitrite actinometry, respectively.  
 329 Photon exposures were ~1.5 - 2 times higher than expected on a clear, October day in Bermuda owing  
 330 to multiple reflections from the aluminum liner used in the water bath. The total exposure time was  
 331 approximately 7 h for each experiment, with the sample exposure interval between 1 and 2 h.  
 332



334

335

336 **Figure 2.** Calculated size-resolved uptake rates of the OH radical and H<sub>2</sub>O<sub>2</sub> into aerosols from  
 337 the gas phase at 80% RH where  $\alpha$  denotes the uptake accommodation coefficient. For  
 338 comparison, mean normalized photochemical production rates of the OH radical and -OOH  
 339 based on irradiated bulk-aerosol extracts are included as horizontal lines (solid line for  $P_{-OOH}$   
 340  $OM+NO_3^-$ , dashed line for  $P_{OH} OM$  acidified and dotted line for  $P_{OH} (OM+NO_3^-)$  acidified).  
 341 For production notation and tabulated normalized rates refer to Table 1. Size-dependent  
 342 variability in *in situ* production rates was not evaluated.